Journal of Pharmaceutical Analysis 11 (2021) 699–708

Contents lists available at ScienceDirect

Journal of Pharmaceutical Analysis

journal homepage: www.elsevier.com/locate/jpa

Original article

Overoxidized poly(3,4-ethylenedioxythiophene)–gold nanoparticles–graphene-modified electrode for the simultaneous detection of dopamine and uric acid in the presence of ascorbic acid

Junqiang Pan [b], Mei Liu [a], Dandan Li [a], Haonan Zheng [a], Dongdong Zhang [a, *]

[a] School of Pharmacy, Xi'an Jiaotong University Health Science Center, Xi'an, 710061, China
[b] Department of Cardiovascular Medicine, Xi'an Central Hospital, Xi'an, 710003, China

ARTICLE INFO

Article history:
Received 10 June 2021
Received in revised form
27 August 2021
Accepted 14 September 2021
Available online 17 September 2021

Keywords:
Graphene
Poly(3,4-ethylenedioxythiophene)
Overoxidation
Dopamine
Uric acid
Ascorbic acid

ABSTRACT

An innovative, ternary nanocomposite composed of overoxidized poly(3,4-ethylenedioxythiophene) (OPEDOT), gold nanoparticles (AuNPs), and electrochemically reduced graphene oxide (ERGO) was prepared on a glassy carbon electrode (GCE) (OPEDOT–AuNPs–ERGO/GCE) through homogeneous chemical reactions and heterogeneous electrochemical methods. The morphology, composition, and structure of this nanocomposite were characterized by transmission electron microscopy, scanning electron microscopy, X-ray diffraction, and X-ray photoelectron spectroscopy. The electrochemical properties of the OPEDOT–AuNPs–ERGO/GCE were investigated by cyclic voltammetry using potassium ferricyanide and hexaammineruthenium(III) chloride redox probe systems. This modified electrode shows excellent electro-catalytic activity for dopamine (DA) and uric acid (UA) under physiological pH conditions, but inhibits the oxidation of ascorbic acid (AA). Linear voltammetric responses were obtained when DA concentrations of approximately 4.0–100 μM and UA concentrations of approximately 20–100 μM were used. The detection limits (S/N=3) for DA and UA were 1.0 and 5.0 μM, respectively, under physiological conditions and in the presence of 1.0 mM of AA. This developed method was applied to the simultaneous detection of DA and UA in human urine, where satisfactory recoveries from 96.7% to 105.0% were observed. This work demonstrates that the developed OPEDOT–AuNPs–ERGO ternary nanocomposite, with its excellent ion-selectivity and electro-catalytic activity, is a promising candidate for the simultaneous detection of DA and UA in the presence of AA in physiological and pathological studies.

1. Introduction

Dopamine (DA) is an essential catecholamine neurotransmitter in the mammalian central nervous system, and its abnormal concentrations induce diverse neurological diseases, like Parkinson's disease and Schizophrenia [1]. Uric acid (UA) is the end product of purine metabolism, and high levels of it have been linked to diseases such as hyperuricemia, gout, and angiocardiopathy [2]. Therefore, the identification and detection of DA and UA have great clinical significance. Since DA and UA possess good electrochemical activities, electrochemical analysis is the preferred approach to identifying these compounds; it also has the added benefits of being simple, rapid, highly sensitive, and inexpensive [3,4]. However, the development of this method is severely restricted by ascorbic acid (AA), which coexists with DA and UA in bodily fluids and interferes with their detection. This is due to AA being present in much higher concentrations than those of DA and UA (approximately 100 to 1,000 times greater) [5]. Hence, specific nanomaterials are desperately needed to modify electrodes for the selective detection of DA and UA and their simultaneous detection in the presence of high concentrations of AA. Materials such as electrodeposited reduced graphene oxide (GO) combined with overoxidized polypyrrole [6], Pt/reduced GO composites [7], carboxyl-functionalized graphene, and silver-nanocube-functionalized polydopamine nanospheres [8] have been successfully employed to prevent AA from reaching electrode surfaces, thus allowing for the individual or simultaneous determination of DA and UA. However, novel electrode-modification materials have yet to be exploited to further improve the analytical performance of DA and UA detection methods.

Peer review under responsibility of Xi'an Jiaotong University.
* Corresponding author.
E-mail address: ddzhang@xjtu.edu.cn (D. Zhang).

https://doi.org/10.1016/j.jpha.2021.09.005

Poly(3,4-ethylenedioxythiophene) (PEDOT) is considered as one of the most promising conducting polymers due to its high conductivity, excellent processability, and exceptional stability. Over the past years, PEDOT has been largely explored for the construction of electrochemical biosensors for environmental monitoring, food and drug analysis, and health care [9]. However, studies employing overoxidized PEDOT (OPEDOT) in electrochemical analysis are rare [10,11]. When exposed to high positive potentials or excess amounts of powerful oxidants, PEDOT can be overoxidized, which causes it to undergo irreversible degradation to give OPEDOT [12–14]. During the overoxidation process, electronegative oxygen groups such as sulfones, carbonyls, and terminal carboxylic groups can be introduced to decrease the hydrophobicity of the OPEDOT film [15], which may endow it with unique properties conducive to electroanalytical applications [9,16]. However, the overoxidation process can also destroy the conjugation of the π-bonds of the PEDOT main chain and lead to unfavorable, low electronic conductivity [13,15]. Therefore, the combination of OPEDOT with other nanomaterials possessing high electronic conductivities and electro-catalytic activities is necessary to compensate for this defect.

Metal nanoparticles, especially gold nanoparticles (AuNPs), have been extensively integrated into PEDOT materials because of their high affinity toward sulfur atoms and their commendable, high specific surface area, catalytic activity, and electrical conductivity [17–19]. PEDOT–AuNPs nanocomposites can be simply and rapidly obtained by the direct chemical reaction between chloroauric acid and the 3,4-ethylenedioxythiophene (EDOT) monomer [20,21]. This one-pot, green synthesis does not require any dispersing agents; however, it usually causes the agglomeration of the nanocomposites, which severely affect the electro-catalytic activity of the resultant nanocomposites [22,23]. There have been reports of nanocomposites based on GO that show good stability and dispersity due to the abundance of hydrophilic groups and the great surface area of GO sheets [24,25]. For example, Liu et al. [26] successfully prepared a stable, aqueous dispersion of PEDOT nanorods that were stabilized by the π–π stacking interactions and electrostatic adsorption between the positively charged PEDOT and negatively charged GO.

Herein, an innovative nanocomposite, OPEDOT–AuNPs–electrochemically reduced GO (ERGO), was prepared by a combination of chemical and electrochemical methods. The PEDOT–AuNPs were first synthesized by a direct, homogeneous, chemical reaction between chloroauric acid (as an oxidant), a source of metal atoms, and the EDOT monomer (as a reductant) at room temperature. Subsequently, GO was added to the PEDOT–AuNPs to form a homogeneous PEDOT–AuNPs–GO suspension, which was then dropped onto the surface of a glassy carbon electrode (GCE) and dried. Finally, this modified electrode was subjected to two heterogeneous electrochemical treatments via cyclic voltammetry that employed different potential windows to electrochemically reduce GO and overoxidize PEDOT. The fabrication procedure of the OPEDOT–AuNPs–ERGO/GCE is illustrated in Scheme 1. In short, this complicated, ternary nanocomposite can be constructed by a green, mild, and highly efficient synthetic strategy. The morphology, composition, and structure of the OPEDOT–AuNPs–ERGO nanocomposite were characterized by transmission electron microscopy (TEM), scanning electron microscopy (SEM), X-ray diffraction (XRD), and X-ray photoelectron spectroscopy (XPS). The electrochemical properties of the modified electrodes were investigated by cyclic voltammetry using potassium ferricyanide ($K_3Fe(CN)_6$) and hexaammineruthenium(III) chloride ($Ru(NH_3)_6Cl_3$) redox probe systems. The electro-catalytic activities of the OPEDOT–AuNPs–ERGO/GCE towards AA, DA, and UA were investigated by cyclic voltammetry under physiological conditions. The analytical properties of the modified electrode towards DA and UA in the presence of high concentrations of AA were investigated by square wave voltammetry. Additionally, the developed method was applied to the simultaneous detection of DA and UA in human urine samples.

2. Experimental

2.1. Reagents and apparatus

GO was purchased from Nanjing XFNANO Materials Tech Co., Ltd. (Nanjing, China), while EDOT, DA, UA, AA, $K_3Fe(CN)_6$, and $Ru(NH_3)_6Cl_3$ were purchased from Sigma-Aldrich (St. Louis, MO, USA). $HAuCl_4$ was purchased from Strem Chemicals, Inc. (Newburyport, MA, USA). All reagents were of analytical grade, and 18.2 MΩ cm Milli-Q water was used throughout the experiments.

The surface morphologies of the nanocomposites were obtained by TEM (JEOL JEM-2100Plus microscope) and SEM (Gemini SEM 500 microscope). The crystal structures were characterized by XRD using a LabX XRD-6100 system (Shimadzu, Kyoto, Japan). The element compositions of the nanocomposites were analyzed by XPS (AXIS ULtrabld instrument; Kratos, Manchester, UK). Electrochemical measurements were obtained using a CHI760 electrochemical workstation with a conventional three-electrode system, where platinum wire served as the auxiliary electrode, a saturated Ag/AgCl electrode was used as the reference electrode, and a bare or modified GCE (diameter=3.0 mm) served as the working electrode. Sodium phosphate buffer saline (PBS; 10 mM, pH=7.4) was used as electrolyte solution.

2.2. Preparation of the modified electrodes

Firstly, 2.7 mL of an ethanol solution of EDOT (10 mM) was added to 15.3 mL of an aqueous $HAuCl_4$ solution (7.0 mM) under rapid stirring for 4 h at room temperature, and dark-blue PEDOT–AuNPs were obtained. In this process, the EDOT monomer was oxidized and polymerized to PEDOT by chloroauric acid, and $HAuCl_4$ was reduced by the EDOT monomer to give the AuNPs. Next, 2.0 mL of an aqueous GO solution (2.0 mg/mL) was mixed with the PEDOT–AuNPs, followed by sonication for 0.5 h to give the PEDOT–AuNPs and a homogeneous GO suspension (PEDOT–AuNPs–GO). Subsequently, 10 μL of PEDOT–AuNPs–GO was dropped onto the clean surface of a GCE and dried with an infrared lamp to give the modified electrode (PEDOT–AuNPs–GO/GCE). The modified electrode was then immersed in 10 mM PBS (pH=7.4) and subjected to cyclic voltammetric scanning from 0.6 to −1.5 V for 3 cycles at a rate of 50 mV/s. This was done to electrochemically reduce GO, which gave the PEDOT–AuNPs–ERGO/GCE. Finally, the PEDOT–AuNPs–ERGO/GCE was placed in 10 mM PBS (pH=7.4) and further treated by cyclic voltammetry between 0.0v and 1.5 V for 12 cycles at a rate of 50 mV/s to electrochemically overoxidize PEDOT, giving the final, desired electrode (OPEDOT–AuNPs–ERGO/GCE).

3. Results and discussion

3.1. The preparation of the OPEDOT–AuNPs–ERGO/GCE

The electrochemical reduction process of the PEDOT–AuNPs–GO/GCE was investigated by cyclic voltammetry from 0.6 to −1.5 V in N_2-saturated, 10 mM PBS (pH=7.4). From Fig. 1A, it can be seen that a broad, irreversible reduction peak appears between approximately −0.9 and −1.5 V during the first cycle, which is ascribed to the irreversible reduction of the GO functional groups [27]. Moreover, this reduction peak disappears

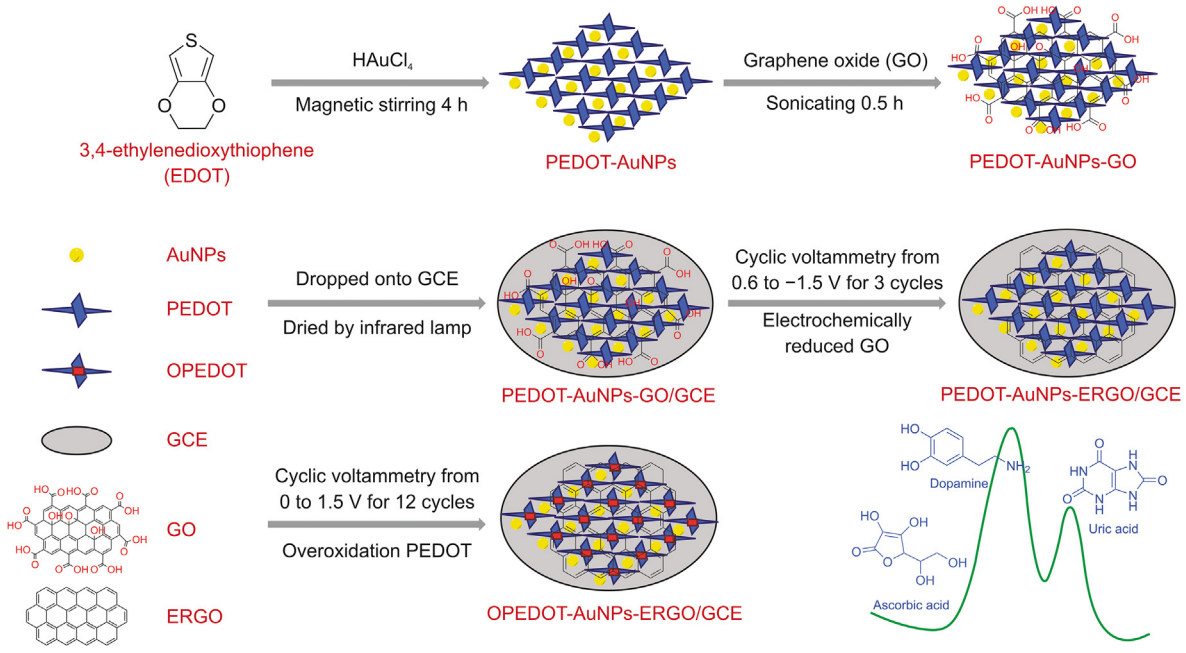

Scheme 1. Schematic diagram of the fabrication procedure of the OPEDOT–AuNPs–ERGO/GCE (OPEDOT: overoxidized poly(3,4-ethylenedioxythiophene); AuNPs: gold nanoparticles; ERGO: electrochemically reduced graphene oxide; GCE: glassy carbon electrode), which was then used to simultaneously detect dopamine (DA) and uric acid (UA) in the presence of ascorbic acid (AA).

during the second and the third cycles, indicating the complete reduction of GO. The electrochemical overoxidation process of the obtained PEDOT–AuNPs–ERGO/GCE was investigated by cyclic voltammetry from 0 to 1.5 V in N_2-saturated, 10 mM PBS (pH=7.4). From Fig. 1B, an irreversible oxidation peak can be seen at approximately 1.1 V during the first cycle. The oxidation peak current was noted to gradually decrease until disappearing as the scan cycles progressed, while the peak potential negatively shifted with increasing scan cycles. This phenomenon might be attributed to the overoxidation of the PEDOT film, which can result in the irreversible degradation of the film and the loss of the electro-activity of PEDOT. Furthermore, an irreversible reduction peak can be seen at approximately 0.52 V, the peak current of which also continuously declined with increasing scan cycles until it disappeared. This irreversible reduction is likely the ion-assisted reduction of the polymer double bonds owing to the presence of alkali metal cations, Na^+ and K^+, in PBS [28].

3.2. The characterization of the OPEDOT–AuNPs–ERGO/GCE

Fig. 2 displays the TEM images of the PEDOT–AuNPs and PEDOT–AuNPs–GO. In Fig. 2A, the AuNPs with a particle size of approximately 5 nm randomly attached to the surface of PEDOT, and a porous network structure can be seen. In Fig. 2B, while GO is introduced, in addition to AuNPs of similar size and PEDOT with porous network structure, PEDOT and AuNPs can also be seen

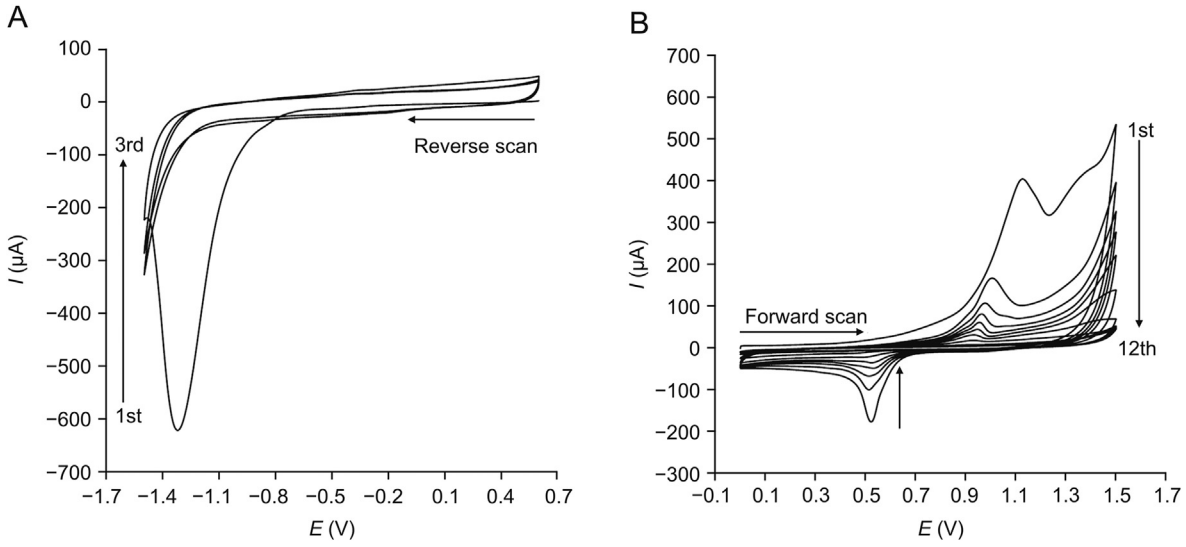

Fig. 1. Cyclic voltammograms of the (A) PEDOT–AuNPs–GO/GCE and (B) PEDOT–AuNPs–ERGO/GCE in N_2-saturated, 10 mM phosphate buffer saline (PBS) (pH=7.4), collected at a scan rate of 50 mV/s.

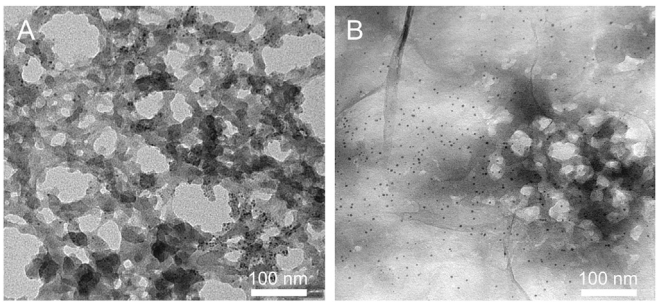

Fig. 2. Transmission electron microscopy (TEM) images of the (A) PEDOT–AuNPs and (B) PEDOT–AuNPs–GO.

adhering to the surface of the wrinkled GO sheets, indicating that GO can provide plenty of deposition sites for both PEDOT and AuNPs.

XRD and XPS were employed to characterize the components of PEDOT–AuNPs–GO. Fig. 3A shows the XRD patterns of GO, the PEDOT–AuNPs, and PEDOT–AuNPs–GO. For GO (curve a), the intense diffraction peak at $2\theta=11.4^{\circ}$ corresponds to the (002) plane of graphite [29]. For the PEDOT–AuNPs (curve b), the diffraction peaks at approximately 38.2°, 45.2°, 65.2°, 78.5°, and 82.8° belong to the (111), (200), (220), (311), and (222) planes of Au, respectively [30]. For PEDOT–AuNPs–GO (curve c), the (002) graphite plane and the typical diffraction peaks of Au can be clearly seen, indicating the simultaneous existence of GO and AuNPs in the nanocomposite. Additionally, a broad peak can be observed in all three curves at 25°, which may correspond to the carbon sources of GO and PEDOT [21]. Fig. 3B shows the XPS spectra of GO and PEDOT–AuNPs–GO. The sharp peaks at 278 and 524 eV are the signals of C1s and O1s, respectively. The high resolution S2p and Au4f spectra of PEDOT–AuNPs–GO are presented in Figs. 3C and D, respectively. From Fig. 3C, the typical peaks of a spin-split doublet can be seen for S2p at 161.1 ($S2p_{3/2}$) and 165.7 eV ($S2p_{1/2}$), which are derived from the thiophene ring of PEDOT. In Fig. 3D, the Au4f spectrum exhibits the $Au4f_{7/2}$ peak at 81.4 eV and the $Au4f_{5/2}$ peak at 85.2 eV. These XRD and XPS characterizations significantly indicate the coexistence of GO, AuNPs, and PEDOT in the fabricated ternary nanocomposite.

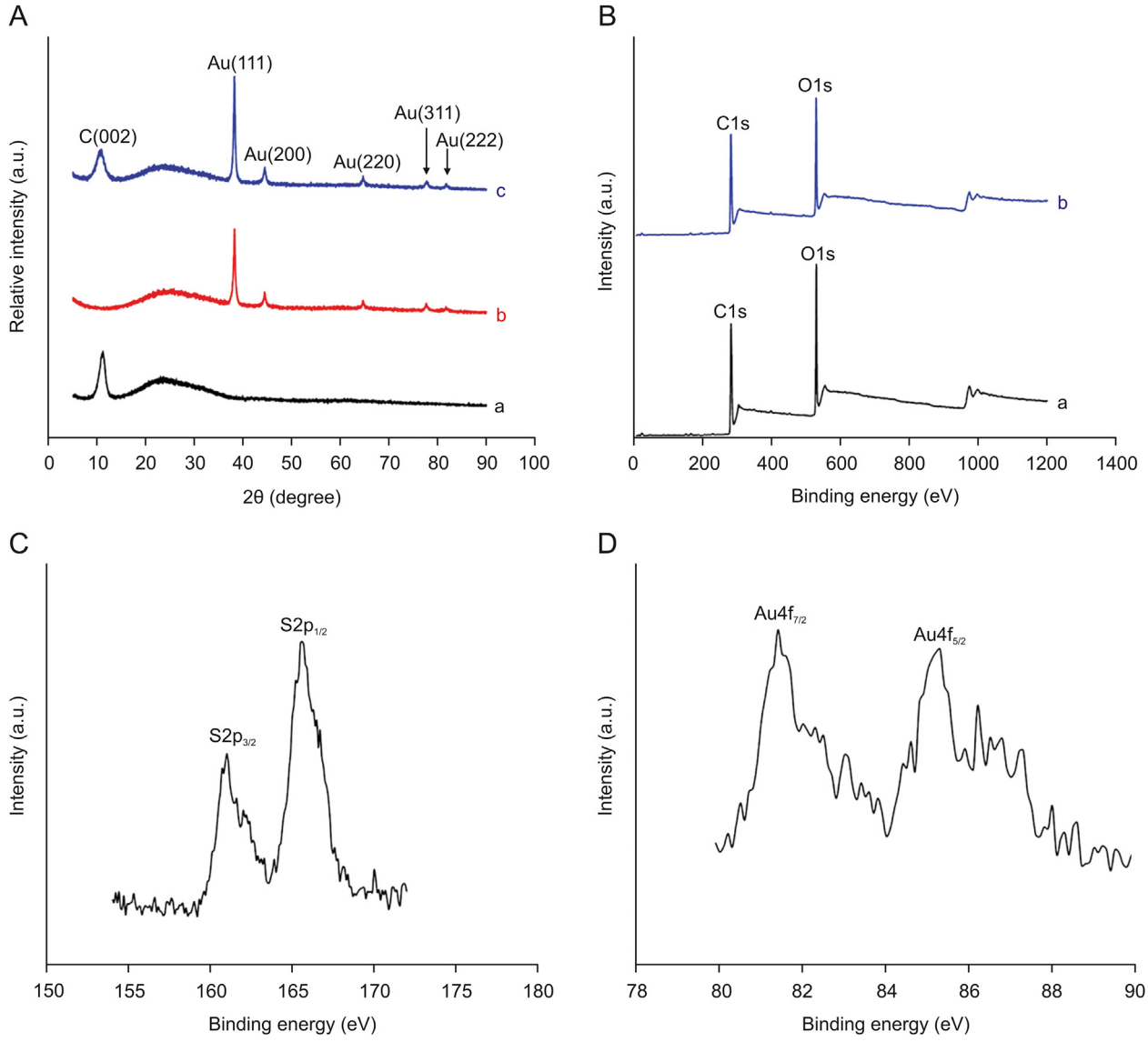

Fig. 3. (A) X-ray diffraction (XRD) patterns of GO (a), the PEDOT–AuNPs (b), and PEDOT–AuNPs–GO (c); (B) X-ray photoelectron spectroscopy (XPS) spectra of GO (a) and PEDOT–AuNPs–GO (b); high resolution (C) S2p and (D) Au4f XPS spectra of PEDOT–AuNPs–GO.

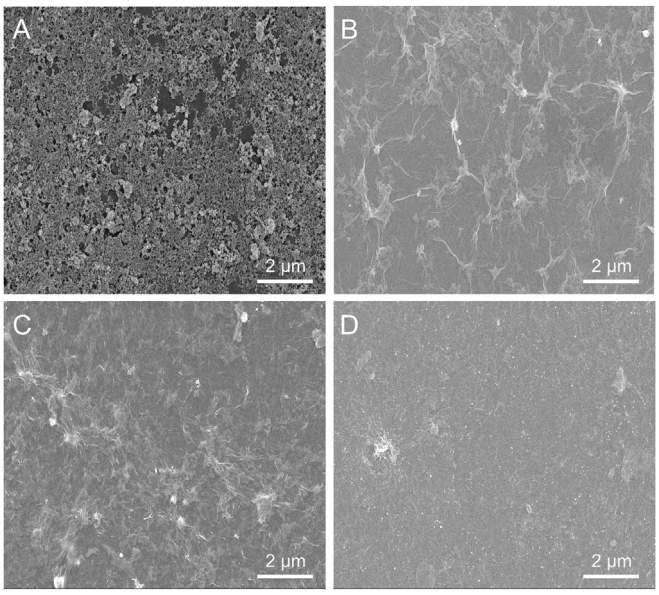

Fig. 4. Scanning electron microscopy (SEM) images of the (A) PEDOT–AuNPs/GCE, (B) PEDOT–AuNPs–GO/GCE, (C) PEDOT–AuNPs–ERGO/GCE, and (D) OPEDOT–AuNPs–ERGO/GCE.

Fig. 4 displays the SEM images of the PEDOT–AuNPs/GCE, PEDOT–AuNPs–GO/GCE, PEDOT–AuNPs–ERGO/GCE, and OPEDOT–AuNPs–ERGO/GCE. In Fig. 4A, the PEDOT–AuNPs can be seen to exhibit a porous, sponge-like structure owing to the involvement of the AuNPs that serve as dopants and templates for the formation and growth of PEDOT [19]. Fig. 4B shows a homogeneous and curly morphology with a thin, wrinkled, paper-like structure. Fig. 4C displays a rough and compact surface with plenty of bulges, which are mainly caused by the electrochemical reduction of GO in the nanocomposites [31]. In Fig. 4D, the bulges almost disappear and the surface becomes relatively flat, which is mainly due to the overoxidation treatment disrupting the thiophene α–α polymer bonds and the PEDOT films being subjected to heavy degradation and delamination [10].

The electrochemical activities of the modified electrodes were investigated in negatively charged $Fe(CN)_6^{3-}$ and positively charged $Ru(NH_3)_6^{3+}$ probe systems, respectively. In the case of the $Fe(CN)_6^{3-}$ system (Fig. 5A), a pair of reversible redox peaks can be seen for the bare GCE (curve a) with the peak potential separation (ΔE_p) being 73 mV and the oxidation peak current (I_{pa}) and reduction peak current (I_{pc}) being 29.0 and −29.7 μA, respectively. For the PEDOT–AuNPs–GO/GCE (curve b), the ΔE_p value broadened to 100 mV, and the I_{pa} and I_{pc} values decreased by 41.9% and 35.0%, respectively. This was probably attributed to the poor electrical conductivity of GO. For the PEDOT–AuNPs–ERGO/GCE (curve c), the value of ΔE_p decreased to 76 mV. Both of the background charge currents and the redox peak currents significantly increased, and the values of I_{pa} and I_{pc} were 29.4 and 38.9 μA, respectively. This suggests that ERGO has a high electrical conductivity and an enhanced ability to accelerate electron transfer [32]. For the OPEDOT–AuNPs–ERGO/GCE (curve d), the background charge currents dramatically decreased, which was due to the cleavage of the conjugation pathway in the PEDOT main chain during the overoxidation process. The values of I_{pa} and I_{pc} decreased to 11.0 and −13.5 μA, respectively, indicating that the electron transfer of the negativity charged $Fe(CN)_6^{3-}$ probe on the electrode surface was impeded due to the electrostatic repulsion of the negatively charged functional groups on the OPEDOT surface.

In the case of the $Ru(NH_3)_6^{3+}$ system (Fig. 5B), a pair of redox peaks appeared for the bare GCE (curve a) with the oxidation peak potential (E_{pa}) being −0.106 V, the reduction peak potential (E_{pc}) being −0.175 V, and the I_{pa} and I_{pc} values being 20.2 and −22.2 μA, respectively. For the PEDOT–AuNPs–GO/GCE (curve b), the E_{pa} and E_{pc} values negatively shifted to −0.132 and −0.206 V, respectively, and the I_{pa} and I_{pc} values increased to 24.3 and −35.0 μA, respectively. This is probably ascribed to the electro-catalytic activity of the AuNPs and the electrostatic adsorption of GO towards $Ru(NH_3)_6^{3+}$. For the PEDOT–AuNPs–ERGO/GCE (curve c), the background charge currents remarkably increased, but the I_{pa} and I_{pc} values decreased to 15.9 and −23.7 μA, respectively. For the OPEDOT–AuNPs–ERGO/GCE (curve d), the oxidation peak split into two sub-peaks at approximately −0.123 and −0.250 V, and the broadened reduction peak negatively shifted to −0.252 V with the I_{pc} value being −26.5 μA. Regarding these two split oxidation peaks,

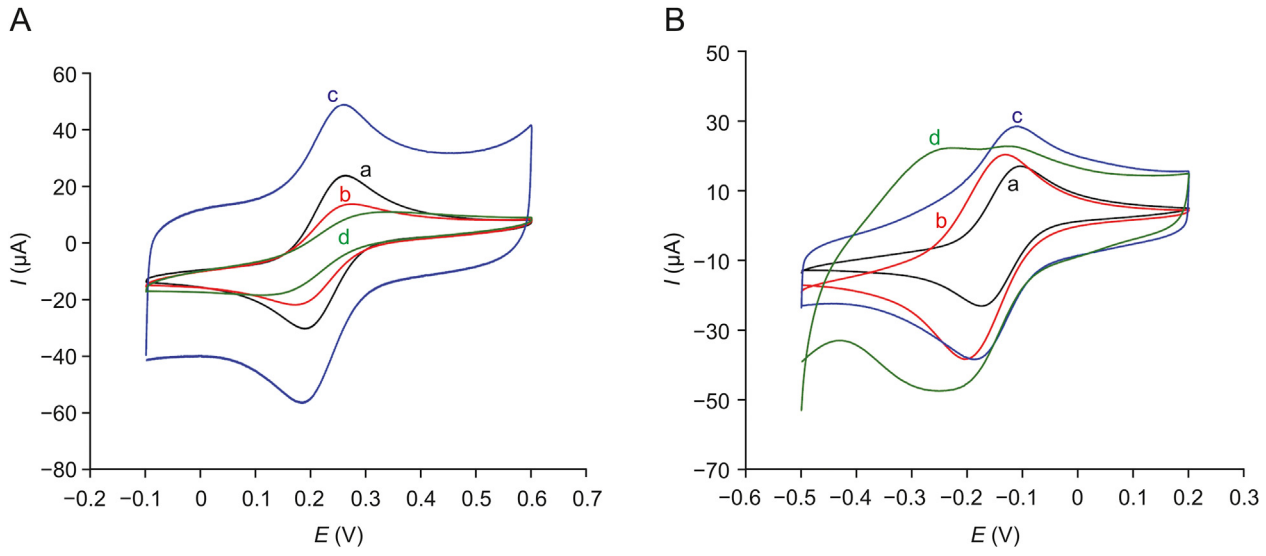

Fig. 5. Cyclic voltammograms obtained in N_2-saturated 10 mM PBS (pH=7.4) containing (A) 2.0 mM $K_3Fe(CN)_6$ and (B) 2.0 mM $Ru(NH_3)_6Cl_3$ on a bare GCE (a), the PEDOT–AuNPs–GO/GCE (b), the PEDOT–AuNPs–ERGO/GCE (c), and the OPEDOT–AuNPs–ERGO/GCE (d), collected at a scan rate of 50 mV/s.

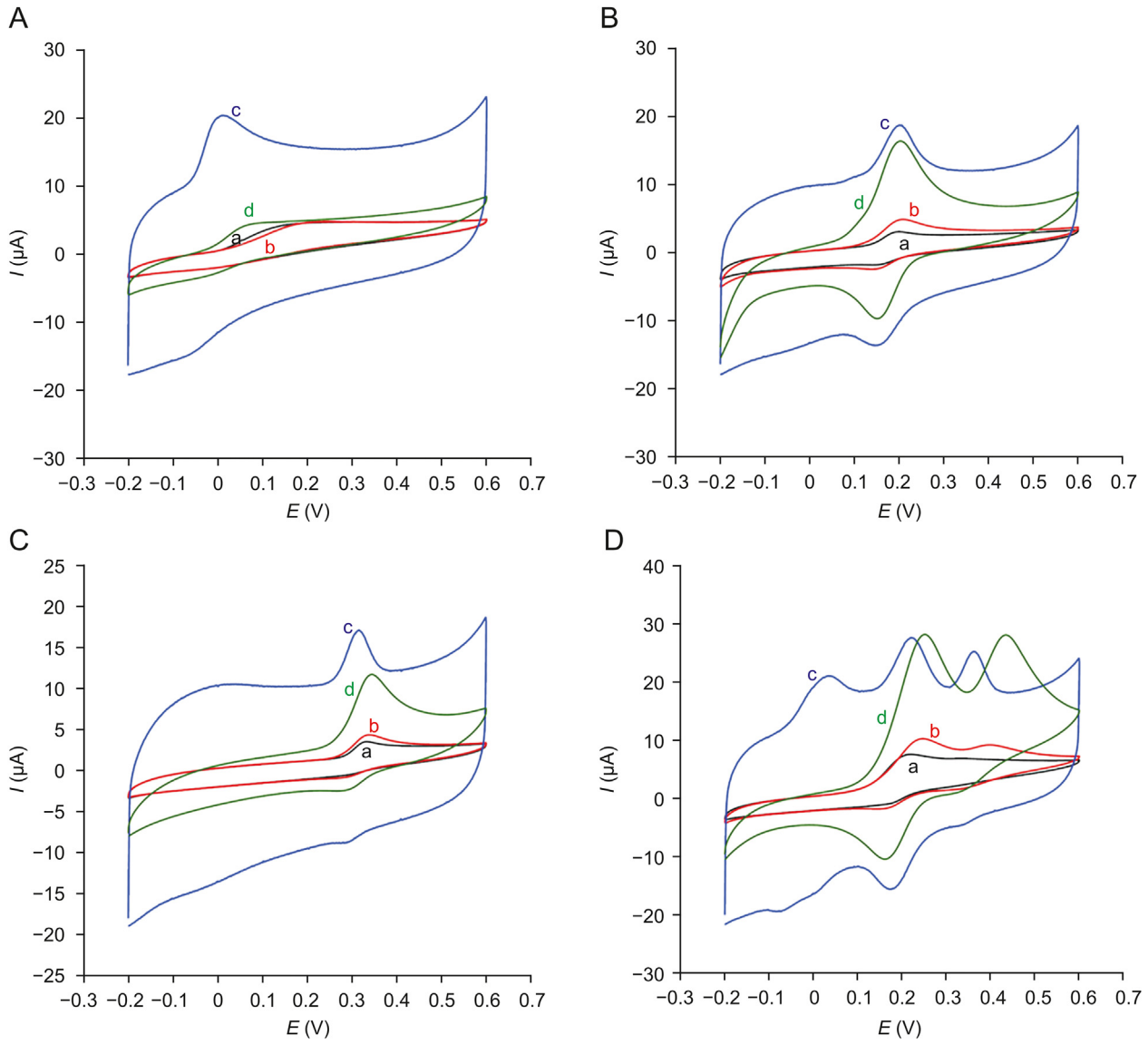

Fig. 6. Cyclic voltammograms of (A) 1.0 mM AA, (B) 0.1 mM DA, (C) 0.1 mM UA, and (D) a mixture of 1.0 mM AA, 0.1 mM DA, and 0.1 mM UA on a bare GCE (a), the PEDOT–AuNPs–GO/GCE (b), the PEDOT–AuNPs–ERGO/GCE (c), and the OPEDOT–AuNPs–ERGO/GCE (d) in 10 mM PBS (pH=7.4), collected at a scan rate of 50 mV/s.

the former wave at $E_{pa} = -0.123$ is ascribed to the oxidation process of liquid-phase $Ru(NH_3)_6^{2+}$ at the electrode surface, while the latter wave at $E_{pa} = -0.250$ V is attributed to the oxidation process of solid-phase $Ru(NH_3)_6^{2+}$ adsorbed onto the electrode surface. Moreover, the broadened reduction peak at −0.252 V is attributed to the merged reduction process of both dissolved and adsorbed $Ru(NH_3)_6^{3+}$ at the electrode surface. This is supported by the cyclic voltammograms (Fig. S1) in which the former wave at −0.123 V was barely observable but the latter wave at −0.250 V was still clearly present when the modified electrode was re-cycled in the pure phosphate buffer in the absence of $Ru(NH_3)_6^{3+}$. These results suggest that the electron transfer of the positively charged $Ru(NH_3)_6^{3+}$ on the electrode surface was promoted due to the strong electrostatic adsorption of negative charged functional groups on the OPEDOT surface.

These electrochemical characterization results reveal that the OPEDOT–AuNPs–ERGO nanocomposite film possesses excellent ion-selectivity. The oxygen-containing sulfone, carbonyl, and carboxylic groups introduced during the overoxidation process were found to hinder the approach of the anion to the electrode surface (for electron transfer) but promote that of the cation. In addition, upon comparing the electrochemical behavior of the OPEDOT–AuNPs–ERGO/GCE with that of the PEDOT–AuNPs–ERGO/GCE in both the $Fe(CN)_6^{3-}$ and $Ru(NH_3)_6^{3+}$ systems, it could be seen that the electrochemical activity of the electrode modification material can be significantly changed through an electrochemical overoxidation process.

3.3. Electrochemical behaviors of AA, DA, and UA on the OPEDOT–AuNPs–ERGO/GCE

The electrochemical catalysis of AA, DA, and UA on the GCE, PEDOT–AuNPs–GO/GCE, PEDOT–AuNPs–ERGO/GCE, and OPEDOT–AuNPs–ERGO/GCE was investigated by cyclic voltammetry. In Fig. 6A, the oxidation peak of AA on a bare GCE (curve a) was observed at +0.144 V, with the peak current being 4.8 μA. The electrochemical behavior of AA on the PEDOT–AuNPs–GO/GCE (curve b) was very similar to that of AA on the bare GCE. For the

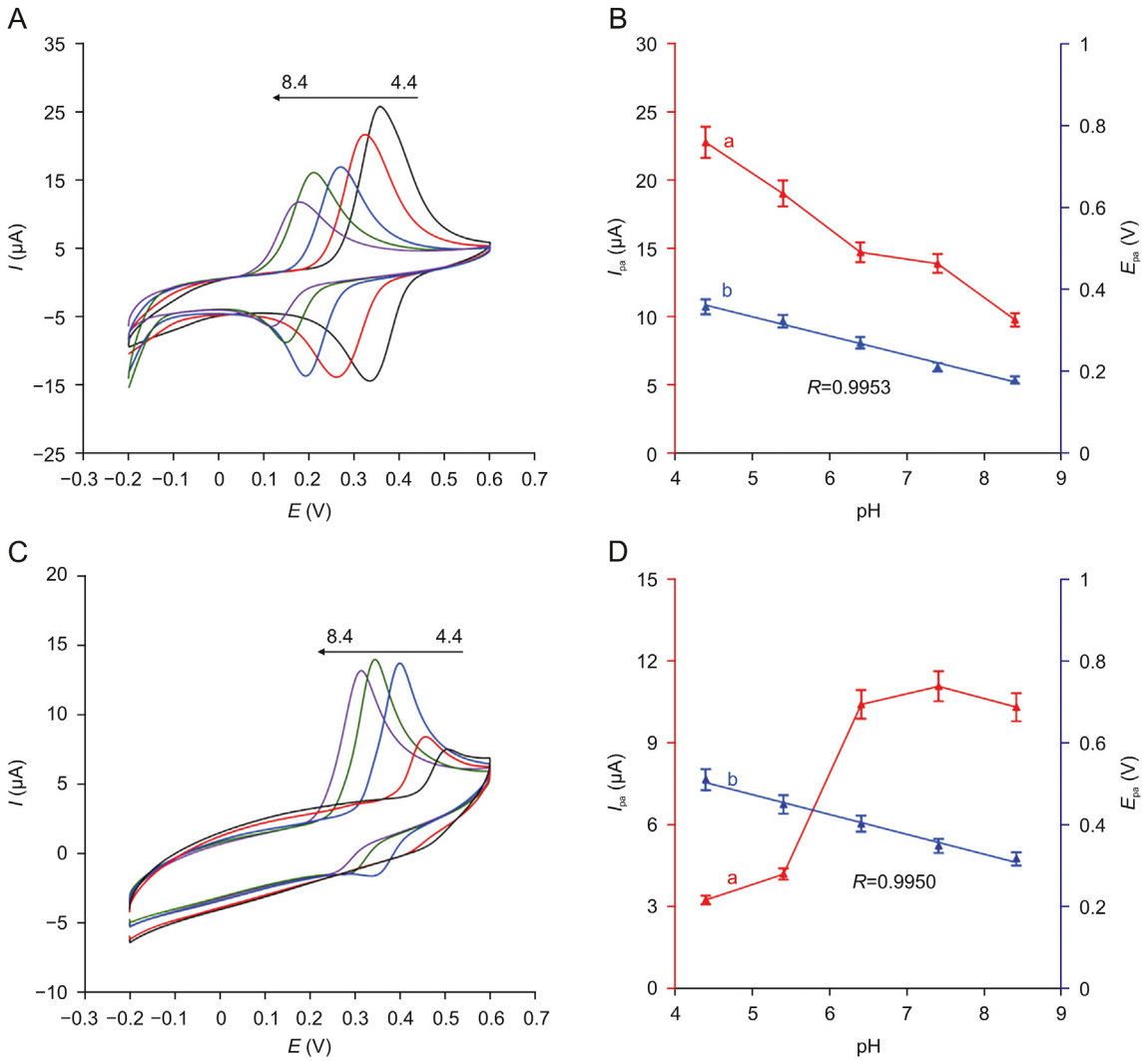

Fig. 7. Cyclic voltammograms and effects of pH on the oxidation peak currents (a) and oxidation peak potentials (b) of (A and B) 0.1 mM DA and (C and D) 0.1 mM UA for the OPEDOT–AuNPs–ERGO/GCE in 10 mM PBS with pH values of 4.4, 5.4, 6.4, 7.4, and 8.4, collected at a scan rate of 50 mV/s.

PEDOT–AuNPs–ERGO/GCE (curve c), the oxidation peak potential negatively shifted to +0.012 V and the oxidation peak current increased to 10.3 μA. For the OPEDOT–AuNPs–ERGO/GCE (curve d), the oxidation peak appeared at +0.077 V and the oxidation peak current dramatically declined to a level comparable to that observed with the bare GCE. This indicates that the OPEDOT–AuNPs–ERGO nanocomposite can effectively block the electron transfer of AA.

In Fig. 6B, DA exhibits a pair of redox peaks at +0.197 and +0.147 V with a ΔE_p value of 50 mV and a formal potential ($E_{1/2}$) of +0.172 V at the bare electrode. The ΔE_p values barely changed when the bare electrode was replaced with the other modified electrodes, but the oxidation peak current at the OPEDOT–AuNPs–ERGO/GCE (12.7 μA) was 6.4, 3.7, and 1.6 times greater than those at the bare GCE (2.0 μA), PEDOT–AuNPs–GO/GCE (3.4 μA), and PEDOT–AuNPs–ERGO/GCE (7.9 μA), respectively. Additionally, the reduction peak current at the OPEDOT–AuNPs–ERGO/GCE (8.0 μA) was 7.3, 4.7, and 1.5 times greater than those at the bare GCE (1.1 μA), PEDOT–AuNPs–GO/GCE (1.7 μA), and PEDOT–AuNPs–ERGO/GCE (5.4 μA), respectively. This suggests that the OPEDOT–AuNPs–ERGO/GCE shows electro-catalytic activity towards DA that is superior to those of the other electrodes.

As shown in Fig. 6C, the oxidation peak current of UA at the OPEDOT–AuNPs–ERGO/GCE (9.7 μA) is 5.3, 3.7, and 1.4 times greater than those at the bare GCE (1.8 μA), PEDOT–AuNPs–GO/GCE (2.6 μA), and PEDOT–AuNPs–ERGO/GCE (6.8 μA), respectively. Furthermore, a weak reduction peak of UA at +0.290 V can be observed when the PEDOT–AuNPs–ERGO/GCE was used. For the OPEDOT–AuNPs–ERGO/GCE, this reduction peak is more intense with a reduction peak current of 1.4 μA, indicating the excellent electrochemical catalytic effect that the OPEDOT–AuNPs–ERGO/GCE has on the electrochemical redox reaction of UA.

In order to further investigate the electro-catalytic activity of OPETOT–AuNPs–ERGO, a system with AA, DA, and UA coexisting was tested by cyclic voltammetry, as shown in Fig. 6D. When the bare GCE was used, it was difficult to distinguish AA, DA, and UA from one another, and only a broad peak was seen at +0.197 V. When the PEDOT–AuNPs–GO/GCE was employed, the oxidation peak of UA was slightly separated from the overlapping oxidation peak corresponding to the other two species. When the PEDOT–AuNPs–ERGO/GCE was used, three well-defined oxidation peaks were observed at approximately +0.034, +0.232, and +0.370 V, corresponding to AA, DA, and UA, respectively. More interestingly, with the OPEDOT–AuNPs–ERGO/GCE, AA did not

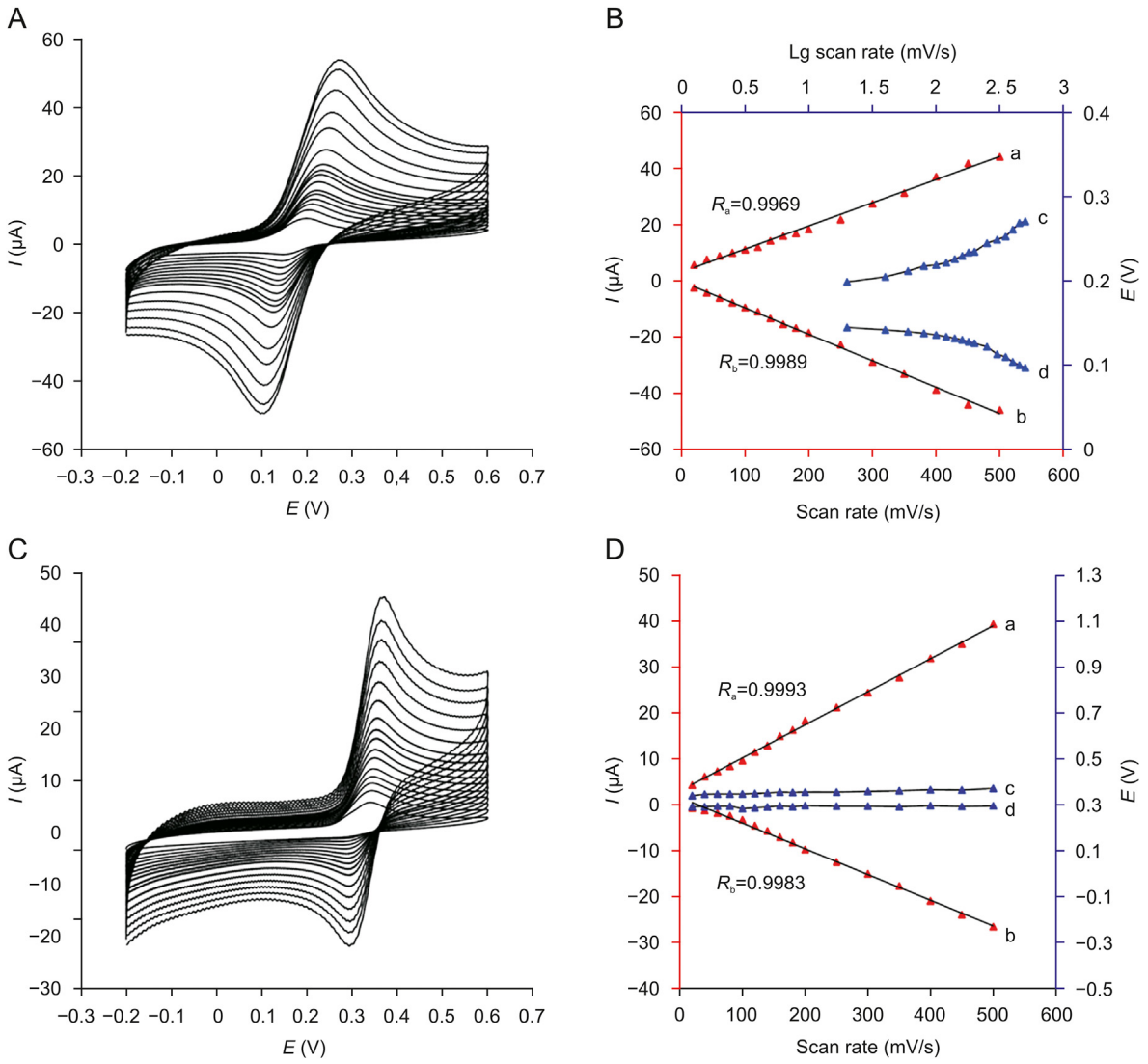

Fig. 8. (A and C) Cyclic voltammograms and (B and D) the plots of peak currents and anodic and cathodic potentials versus scan rate on the OPEDOT–AuNPs–ERGO/GCE in 10 mM PBS (pH=7.4) containing (A and B) 0.1 mM DA and (C and D) 0.1 mM UA at different scan rates (from inner to outer): 20, 40, 60, 80, 100, 120, 140, 160, 180, 200, 250, 300, 350, 400, 450, and 500 mV/s. Lines a and b are the plots of the peak currents, and lines c and d are the plots of the peak potentials versus scan rate or the log of scan rate.

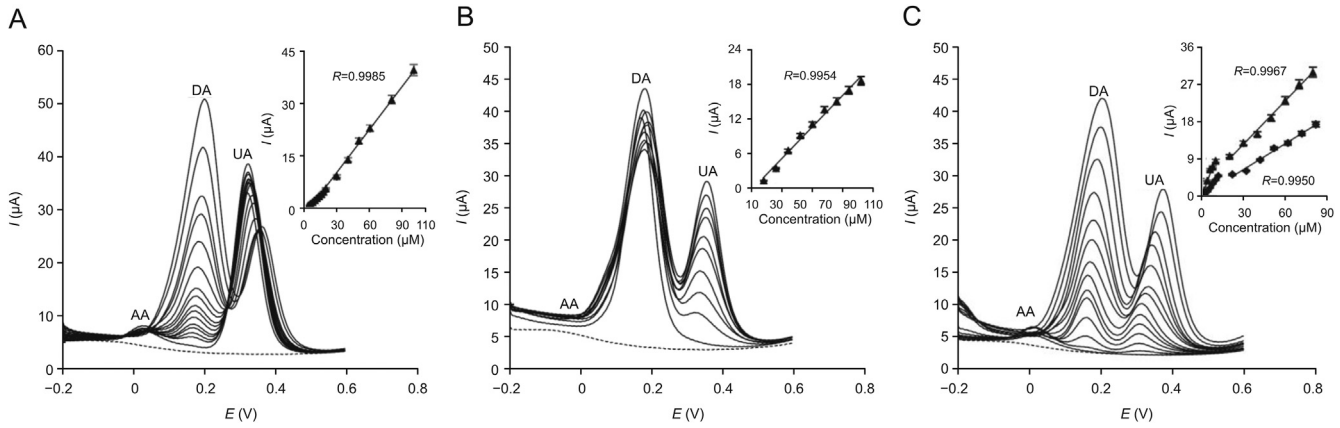

Fig. 9. Square wave voltammograms of DA and UA on the OPEDOT–AuNPs–ERGO/GCE in 10 mM PBS pH=7.4, collected at a scan rate of 50 mV/s. (A) DA concentrations of 0, 4.0, 6.0, 8.0, 10, 12, 14, 16, 18, 20, 30, 40, 50, 60, 80, and 100 μM in the presence of 1,000 μM AA and 100 μM UA; (B) UA concentrations of 0, 20, 30, 40, 50, 60, 70, 80, 90, and 100 μM in the presence of 0.5 mM AA and 50 μM DA. (C) DA concentrations of 0.0, 1.0, 2.0, 4.0, 6.0, 8.0, 10, 20, 30, 40, 50, 60, 70, and 80 μM and UA concentrations of 0, 2.0, 4.0, 6.0, 8.0, 10, 12, 22, 32, 42, 52, 62, 72, and 82 μM in the presence of 0.5 mM AA. The insets show the linear relationships between the currents and concentrations of DA and UA.

exhibit an obvious electrochemical response, while the oxidation peaks of DA and UA could be clearly seen at +0.257 and +0.436 V, respectively, which is in accordance with the behavior of AA without UA and DA present, as can be seen in Fig. 6A. These results demonstrate that the OPEDOT–AuNPs–ERGO/GCE has excellent electrocatalysis and selectivity towards DA and UA, which is mainly attributed to the increased hydrophilicity of the film, the electronegativity of the abundant oxygen groups of OPEDOT, the electrocatalytic activity of graphene and the AuNPs, as well as the synergetic effects among these nanomaterials. Hence, the electrochemical performance and application of the OPEDOT–AuNPs–ERGO/GCE in the selective and sensitive determination of DA and UA in the presence of AA are worthy of exploration.

The effects of pH on the anodic peak currents and peak potentials of DA and UA at the OPEDOT–AuNPs–ERGO/GCE were investigated by cyclic voltammetry in 10 mM PBS solutions with pH values ranging from 4.4 to 8.4. From Fig. 7, it can be seen that the oxidation peak currents of DA decrease with an increase in pH, while the oxidation peak currents of UA increase with increasing pH. This can be attributed to the fact that the amino group of DA receives a positive charge under acidic conditions because the pK_b of DA is 8.87, whereas UA possesses a neutral and an anionic charge under the same conditions because the pK_a of UA is 5.76 [33]. However, a pH of 7.4 was still chosen for the supporting electrolyte in the following electrochemical measurements to reflect physiological pH. Both the redox peak potentials negatively shifted with increasing pH, and the oxidation peak potentials of DA and UA exhibited good linear relationships with pH; the linear regression equations are E_{pa} (V) = 0.57–0.047 × pH (R = 0.9953) and E_{pa} (V) = 0.71–0.049 × pH (R = 0.9950) for DA and UA, respectively. The corresponding slopes of 47 and 49 mV/pH, for DA and UA, respectively, are close to the theoretical value of 59 mV/pH. This indicates that an equal number of electron and proton transfer processes occur with both DA and UA [34].

The kinetics of the electrode reaction was investigated by exploring the dependence of the redox peak currents of DA and UA on the scan rate. Fig. 8 shows the cyclic voltammograms of the OPEDOT–AuNPs–ERGO/GCE in 10 mM PBS with scan rates ranging from 20 to 500 mV/s. From Figs. 8 A and B, it can be seen that both the absolute values of the oxidation and reduction peak currents linearly increase with increasing scan rate. The absolute values of the redox peak potentials increased with the log of the scan rate, remained nearly constant at low scan rates, and linearly increased at high scan rates. This indicates that the electrochemical process of DA at the OPEDOT–AuNPs–ERGO/GCE is a surface-confined process with relatively slow electron transfer [6,35]. From Figs. 8C and D, it can be seen that both the absolute values of the oxidation and reduction peak currents linearly increase with increasing scan rate, while the peak potentials remain nearly unchanged with increasing scan rate. This indicates that the electrochemical process of UA at the OPEDOT–AuNPs–ERGO/GCE is a surface-confined process with fast electron transfer [36].

3.4. Simultaneous determination of DA and UA in the presence of AA

Fig. 9 shows the square wave voltammograms at the OPEDOT–AuNPs–ERGO/GCE for the different concentrations of DA and UA in 10 mM PBS (pH=7.4) in the presence of AA. In Fig. 9A, the oxidation peak currents can be seen to increase linearly as the DA concentration was increased from 4.0 to 100 μM. This was in the presence of 1.0 mM AA and 100 μM UA, and the corresponding linear equation is I_{pa} (μA) = 0.41 × C_{DA} (μM) − 2.1 (R = 0.9985). From Fig. 9B, the oxidation peak currents can be seen to increase linearly as the UA concentration was increased from 20 to 100 μM. This was in the presence of 0.5 mM AA and 50 μM DA, and the corresponding linear equation is I_{pa} (μA) = 0.22 × C_{UA} (μM) − 2.5 (R = 0.9954). The corresponding detection limits (S/N=3) were 1.0 μM for DA and 5.0 μM for UA. From Fig. 9C, it can be seen that the oxidation peak currents increase linearly with the concentrations of DA and UA in the presence of 0.5 mM AA. For DA, the corresponding linear equations are I_{pa} (μA) = 0.94 × C_{DA} (μM) − 0.27 (R = 0.9826) in the range of 1.0–10 μM and I_{pa} (μA) = 0.35 × C_{DA} (μM) − 2.1 (R = 0.9967) in the range of 20–80 μM. For UA, the corresponding linear equations are I_{pa} (μA) = 0.46 × C_{UA} (μM) − 0.65 (R = 0.9993) in the range of 2.0–12 μM and I_{pa} (μA) = 0.21 × C_{UA} (μM) + 0.18 (R = 0.9950) in the range of 22–82 μM.

Moreover, this modified electrode was successfully applied to the detection of DA and UA in human urine samples, which were diluted 250 times with 10 mM PBS (pH=7.4) before the measurements. When known amounts of DA and UA were added to the human urine samples, satisfactory, quantitative recoveries were obtained for both DA (96.7%–105.0%) and UA (98.7%–100.8%) (as shown in Table S1). This indicates the potential of the OPEDOT–AuNPs–ERGO/GCE to be used for the detection of DA and UA in the presence of AA under physiological and pathological conditions.

4. Conclusion

A novel, graphene-based, ternary composite, OPEDOT–AuNPs–ERGO, was prepared on a GCE to give a modified electrode (OPEDOT–AuNPs–ERGO/GCE) that was successfully applied to the simultaneous determination of DA and UA in the presence of AA under physiological pH conditions. This work demonstrates that the developed OPEDOT–AuNPs–ERGO/GCE displays electro-catalytic activities towards the redox reactions of UA and DA that are superior to those of other electrodes evaluated. This electrode also inhibited the oxidation of AA. It is worth noting that the electrochemical activity of the electrode modification material can be significantly changed through an electrochemical overoxidation process. Additionally, OPEDOT facilitated analytical application despite the overoxidation process resulting in mechanical degradation and decreased electronic conductivity. This work reveals that OPEDOT–AuNPs–ERGO, with its attractive features, is a promising candidate for electroanalytical and clinical applications.

Declaration of competing interest

The authors declare that there are no conflicts of interest.

Acknowledgments

Financial supports from the Natural Science Foundation of Shaanxi Province, China (Grant No.: 2020JM-652), Fundamental Research Funds for the Central Universities of Xi'an Jiaotong University (Grant No.: xzy012020054), and Cultivation Project of Xi'an Health Committee (Grant No.: 2020MS02) are gratefully acknowledged.

Appendix A. Supplementary data

Supplementary data to this article can be found online at https://doi.org/10.1016/j.jpha.2021.09.005.

References

[1] M.O. Klein, D.S. Battagello, A.R. Cardoso, et al., Dopamine: functions, signaling,

and association with neurological diseases, Cell. Mol. Neurobiol. 39 (2019) 31–59.
[2] J. Maiuolo, F. Oppedisano, S. Gratteri, et al., Regulation of uric acid metabolism and excretion, Int. J. Cardiol. 213 (2016) 8–14.
[3] S.I. Kaya, S. Kurbanoglu, S.A. Ozkan, Nanomaterials-based nanosensors for the simultaneous electrochemical determination of biologically important compounds: ascorbic acid, uric acid, and dopamine, Crit. Rev. Anal. Chem. 49 (2019) 101–125.
[4] T. Xiao, F. Wu, J. Hao, et al., In vivo analysis with electrochemical sensors and biosensors, Anal. Chem. 89 (2017) 300–313.
[5] D. Li, M. Liu, Y. Zhan, et al., Electrodeposited poly(3,4-ethylenedioxythiophene) doped with graphene oxide for the simultaneous voltammetric determination of ascorbic acid, dopamine and uric acid, Microchim. Acta 187 (2020), 94.
[6] X. Chen, D. Li, W. Ma, et al., Preparation of a glassy carbon electrode modified with reduced graphene oxide and overoxidized electropolymerized polypyrrole, and its application to the determination of dopamine in the presence of ascorbic acid and uric acid, Microchim. Acta 186 (2019), 407.
[7] T.Q. Xu, Q.L. Zhang, J.N. Zheng, et al., Simultaneous determination of dopamine and uric acid in the presence of ascorbic acid using Pt nanoparticles supported on reduced graphene oxide, Electrochim. Acta 115 (2014) 109–115.
[8] Y. Li, Y. Jiang, Y. Song, et al., Simultaneous determination of dopamine and uric acid in the presence of ascorbic acid using a gold electrode modified with carboxylated graphene and silver nanocube functionalized polydopamine nanospheres, Microchim. Acta 185 (2018), 382.
[9] Y. Hui, C. Bian, S. Xia, et al., Synthesis and electrochemical sensing application of poly(3,4-ethylenedioxythiophene)-based materials: a review, Anal. Chim. Acta 1022 (2018) 1–19.
[10] J.M. Lin, Y.L. Su, W.T. Chang, et al., Strong adsorption characteristics of a novel overoxidized poly(3,4-ethylenedioxythiophene) film and application for dopamine sensing, Electrochim. Acta 149 (2014) 65–75.
[11] A. Özcan, S. İlkbas, Preparation of poly(3,4-ethylenedioxythiophene) nanofibers modified pencil graphite electrode and investigation of over-oxidation conditions for the selective and sensitive determination of uric acid in body fluids, Anal. Chim. Acta 891 (2015) 312–320.
[12] X. Du, Z. Wang, Effects of polymerization potential on the properties of electrosynthesized PEDOT films, Electrochim. Acta 48 (2003) 1713–1717.
[13] A. Zykwinska, W. Domagala, B. Pilawa, et al., Electrochemical overoxidation of poly(3,4-ethylenedioxythiophene)—PEDOT studied by means of in situ ESR spectroelectrochemistry, Electrochim. Acta 50 (2005) 1625–1633.
[14] Y. Hui, C. Bian, J. Wang, et al., Comparison of two types of overoxidized PEDOT films and their application in sensor fabrication, Sensors (Basel) 17 (2017), 628.
[15] P. Tehrani, A. Kanciurzewska, X. Crispin, et al., The effect of pH on the electrochemical over-oxidation in PEDOT:PSS films, Solid State Ionics 177 (2007) 3521–3527.
[16] L.V. Kayser, D.J. Lipomi, Stretchable conductive polymers and composites based on PEDOT and PEDOT:PSS, Adv. Mater. 31 (2019), e1806133.
[17] K. Krukiewicz, M. Chudy, S. Gregg, et al., The synergistic effects of gold particles and dexamethasone on the electrochemical and biological performance of PEDOT neural interfaces, Polymers (Basel) 11 (2019), 67.
[18] L. Yang, J. Zhang, F. Zhao, et al., Electrodeposition of self-assembled poly(3,4-ethylenedioxythiophene) @gold nanoparticles on stainless steel wires for the headspace solid-phase microextraction and gas chromatographic determination of several polycyclic aromatic hydrocarbons, J. Chromatogr. A 1471 (2016) 80–86.
[19] P. Lin, F. Chai, R. Zhang, et al., Electrochemical synthesis of poly(3,4-ethylenedioxythiophene) doped with gold nanoparticles, and its application to nitrite sensing, Microchim. Acta 183 (2016) 1235–1241.
[20] P. Xu, X. Han, B. Zhang, et al., Multifunctional polymer-metal nanocomposites via direct chemical reduction by conjugated polymers, Chem. Soc. Rev. 43 (2014) 1349–1360.
[21] Z. Liu, J. Xu, R. Yue, et al., Facile one-pot synthesis of Au–PEDOT/rGO nanocomposite for highly sensitive detection of caffeic acid in red wine sample, Electrochim. Acta 196 (2016) 1–12.
[22] L. Gao, R. Yue, J. Xu, et al., Pt-PEDOT/rGO nanocomposites: one-pot preparation and superior electrochemical sensing performance for caffeic acid in tea, J. Electroanal. Chem. 816 (2018) 14–20.
[23] F. Jiang, R. Yue, Y. Du, et al., A one-pot 'green' synthesis of Pd-decorated PEDOT nanospheres for nonenzymatic hydrogen peroxide sensing, Biosens. Bioelectron. 44 (2013) 127–131.
[24] G. Xu, Z.A. Jarjes, V. Desprez, et al., Sensitive, selective, disposable electrochemical dopamine sensor based on PEDOT-modified laser scribed graphene, Biosens. Bioelectron. 107 (2018) 184–191.
[25] H.C. Tian, J.Q. Liu, D.X. Wei, et al., Graphene oxide doped conducting polymer nanocomposite film for electrode-tissue interface, Biomaterials 35 (2014) 2120–2129.
[26] S. Liu, J. Tian, L. Wang, et al., Production of stable aqueous dispersion of poly(3,4-ethylenedioxythiophene) nanorods using graphene oxide as a stabilizing agent and their application for nitrite detection, Analyst 136 (2011) 4898–4902.
[27] Z. Wang, X. Zhou, J. Zhang, et al., Direct electrochemical reduction of single-layer graphene oxide and subsequent functionalization with glucose oxidase, J. Phys. Chem. C 113 (2009) 14071–14075.
[28] G. Zotti, G. Schiavon, S. Zecchin, Irreversible processes in the electrochemical reduction of polythiophenes. Chemical modifications of the polymer and charge-trapping phenomena, Synth. Met. 72 (1995) 275–281.
[29] Y. Xu, H. Bai, G. Lu, et al., Flexible graphene films via the filtration of water-soluble noncovalent functionalized graphene sheets, J. Am. Chem. Soc. 130 (2008) 5856–5857.
[30] S. Khan, M. Ul-Islam, M.W. Ullah, et al., Nano-gold assisted highly conducting and biocompatible bacterial cellulose-PEDOT:PSS films for biology-device interface applications, Int. J. Biol. Macromol. 107 (2018) 865–873.
[31] W. Wang, G. Xu, X.T. Cui, et al., Enhanced catalytic and dopamine sensing properties of electrochemically reduced conducting polymer nanocomposite doped with pure graphene oxide, Biosens. Bioelectron. 58 (2014) 153–156.
[32] D. Zhang, X. Chen, W. Ma, et al., Direct electrochemistry of glucose oxidase based on one step electrodeposition of reduced graphene oxide incorporating polymerized l-lysine and its application in glucose sensing, Mat. Sci. Eng. C-Mater. 104 (2019), 109880.
[33] B. Dinesh, A.T.E. Vilian, C.H. Kwak, et al., The facile and simple synthesis of poly(3,4ethylenedioxythiophene) anchored reduced graphene oxide nanocomposite for biochemical analysis, Anal. Chim. Acta 1077 (2019) 150–159.
[34] D. Zhang, L. Li, W. Ma, et al., Electrodeposited reduced graphene oxide incorporating polymerization of l-lysine on electrode surface and its application in simultaneous electrochemical determination of ascorbic acid, dopamine and uric acid, Mater. Sci. Eng. C Mater. Biol. Appl. 70 (2017) 241–249.
[35] D. Zhang, L. Fu, L. Liao, et al., Electrochemically functional graphene nanostructure and layer-by-layer nanocomposite incorporating adsorption of electroactive methylene blue, Electrochim. Acta 75 (2012) 71–79.
[36] A.J. Bard, L.R. Faulkner, Electrochemical Methods: Fundamentals and Applications, Wiley, New York, 2001.